

Finite Josephson junction arrays with open boundaries in magnetic field: Ground state energy and first critical field

D.E. Shalóm, J.S. Reparaz, and H. Pastoriza^a

Centro Atómico Bariloche and Instituto Balseiro, Comisión Nacional de Energía Atómica, R8402AGP S.C. de Bariloche, Argentina

Received 15 December 2003

Published online 13 July 2004 – © EDP Sciences, Società Italiana di Fisica, Springer-Verlag 2004

Abstract. We have investigated the size dependence of the ground state energy as a function of the magnetic field in Josephson junction arrays with open boundaries. We present a simple *rings* model that reproduces with great confidence the size and field dependence of the energy of the system obtained by numerical simulation of the Hamiltonian. From these results we obtained the size dependence of the first penetration field, where the one-vortex state becomes favorable compared to the zero-vortex state.

PACS. 74.81.Fa Josephson junction arrays and wire networks

1 Introduction

Josephson junctions have been vastly studied for a number of years as paradigmatic systems for studying phase transitions in two dimensions [1], model high temperature superconductors [2], and studying quantum transitions [3]. The technological ability to fabricate these structures of high quality and the possibility to make numerical simulations of model systems have fostered its study. However, most of the large quantity of publications related with this subject were concentrated in infinite systems. In numerical simulations periodic or quasi-periodic boundary conditions were used to obtain the thermodynamic limit. For example the vortex density induced in a sample is directly determined by the applied magnetic field. On the other hand, all experiments are performed in samples of finite size mostly with open boundaries where size effects hardly could be neglected. Transport measurements involving vortex motion across the samples is strongly affected by vortex–boundary interaction that generates a “surface” barrier [4] or could induce vortex reflection at the sample border [5].

In this regard a number of relevant questions arise: Which would be the equilibrium vortex density in a finite system for a given applied magnetic field? Which would be its structure? Is there a range of fields where a “*Meissner*” phase without vortices in the sample would exist?

In this work we concentrate in the last question. We have calculated analytical and numerically the ground state of finite square Josephson junction arrays as a function of the magnetic field without and with one vortex in

the array. From these calculations we obtain a *first vortex penetration field* as a function of the sample size.

2 Model

The energy for a single Josephson junction between two superconducting electrodes, i, j , without taking into account the electrostatic energy can be written as:

$$E_J(i, j) = \frac{\hbar I_c}{2e} (1 - \cos(\gamma_{i,j})) \quad (1)$$

where $\gamma_{i,j} = \left(\theta_i - \theta_j - \frac{2e}{\hbar c} \int_i^j \mathbf{A} \cdot d\mathbf{l}\right)$ is the gauge invariant phase difference between electrodes, and I_c is the critical current of the junction, e is the electron charge, and \mathbf{A} is the magnetic vector potential.

The Hamiltonian for a network of junctions can be expressed as:

$$H_{JJA} = \frac{1}{2} \sum_{i,\langle j \rangle} E_J(i, j) \quad (2)$$

where i spawns to all sites of array and $\langle j \rangle$ to all nearest neighbors of i . In this model Hamiltonian the capacitive and inductive contributions are neglected.

We are interested in the behavior of finite arrays, which implies that there are superconducting islands located in the perimeter that have less neighbor islands than those located in the interior of the array. In these circumstances the ground state of the system in the presence of a perpendicular magnetic field can not be described by a Bravais lattice of vortices as in infinite systems [6].

^a e-mail: hernan@cab.cnea.gov.ar

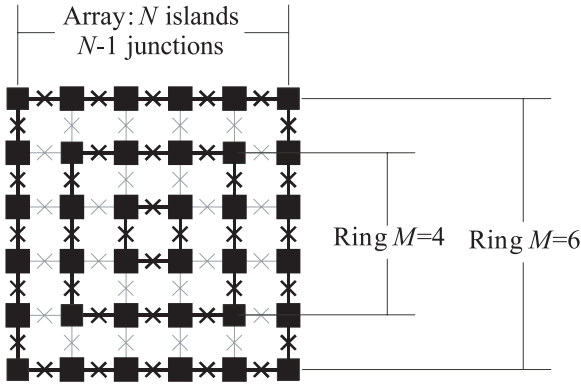


Fig. 1. Sketch of a square Josephson array. Rings taken in the model are emphasized.

2.1 Rings approximation

It is known that in the presence of a magnetic field Meissner currents flow through the perimeter of a superconducting sample, decaying towards the center of the sample. The simplest model that can take the energy cost associated with this “shielding” currents into account is assuming that they flow concentrically mirroring the perimeter of the sample as sketched in Figure 1. With this concentric rings approximation the current that flows in all the junctions of each ring ($I_{i,j} = I_c \sin(\gamma_{i,j})$) is the same, therefore all the $\gamma_{i,j}$ must be identical within each ring. To calculate the $\gamma_{i,j}$ we use the fluxoid quantification:

$$\sum_{\text{ring}} \gamma_{i,j} = 2\pi \frac{\Phi}{\Phi_0} + 2\pi n_v \quad (3)$$

$$= 2\pi f(M-1)^2 + 2\pi n_v \quad (4)$$

where f is the frustration of the array defined as the ratio between the magnetic flux per plaquette and the elementary flux quantum $f = \frac{\Phi E}{\Phi_0}$, n_v indicates the number of vortices concatenated by the ring, and M is the number of superconducting islands in each side of the square ring. As all the $\gamma_{i,j} = \gamma_0$ are equal, the left hand part of equation (3) is equivalent to $4(M-1)\gamma_0$. In this way the energy for a ring of side M is given by:

$$E_{\text{ring}}(M) = 4E_{J0}(M-1) \left\{ 1 - \cos \left[\frac{\pi}{2} \left(f(M-1) + \frac{n_v}{(M-1)} \right) \right] \right\} \quad (5)$$

where we have defined $E_{J0} = \frac{\hbar I_c}{2e}$.

Finally the total energy for a sample of size $N \times N$ can be written as:

$$E_T(n_v, f) = E_{J0} \sum_{k=1}^{N/2} 4(2k-1) \left\{ 1 - \cos \left[\frac{\pi}{2} \left(f(2k-1) + \frac{n_v}{2k-1} \right) \right] \right\}. \quad (6)$$

2.1.1 Zero vortex state

Equation (6) can be approximated in the case of no vortices in the sample and small magnetic fields ($f \ll 1/N$) as:

$$\begin{aligned} E_T(n_v = 0, f) &\approx E_{J0} \sum_{k=1}^{N/2} 4(2k-1) \left[\frac{\pi^2}{8} f^2 (2k-1)^2 \right] \\ &= E_{J0} \frac{\pi^2}{16} (N^4 - 2N^2) f^2. \end{aligned} \quad (7)$$

This expression explicits the quadratic dependence on field of the energy with a curvature proportional to N^4 .

2.1.2 One vortex state

In order to calculate the first penetration field we have to compare the energy of the state calculated in the previous section with that of the state with one vortex in the system.

For the evaluation of the energy of the system with one vortex located in the center of the array we can approximate equation (6) by: $E_T(n_v = 1, f)/E_{J0} \approx a + bf + cf^2$. The first term of this equation corresponds to the energy cost for the creation of a vortex excitation in the system and is function of the size of the sample, $a \propto \log(N/2)$ [7]. The linear and quadratic coefficients can be evaluated through the derivatives of equation (6) given by:

$$b = \frac{\pi^2}{4} N^2 \quad (8)$$

$$c = \frac{\pi^2}{16} (N^4 - 2N^2).$$

Given that the quadratic term of the one vortex configuration is the same as in the “Meissner” state, the first critical field can be easily computed as $f_{C1} = -a/b$, with the a, b previously defined.

3 Numerical results

We have performed numerical simulations of finite arrays to calculate the ground state energy as a function of magnetic field and sample size. We have used a Metropolis algorithm in order to find the global energy minimum of equation (2) in arrays of junctions with square symmetry. In the absence of vortices in the sample we started at zero applied field and all phases equal (which is the ground state of the system), then we change the frustration (magnetic field) in steps of typically $\Delta f = 0.001$, and let the system relax to the minimal energy configuration. This final state was used as seed for the following calculated frustration. In each step we computed the vorticity of the system to check that no vortices were present in the obtained phase configuration. In Figure 2 we plot the total energy as a function of frustration for various sample

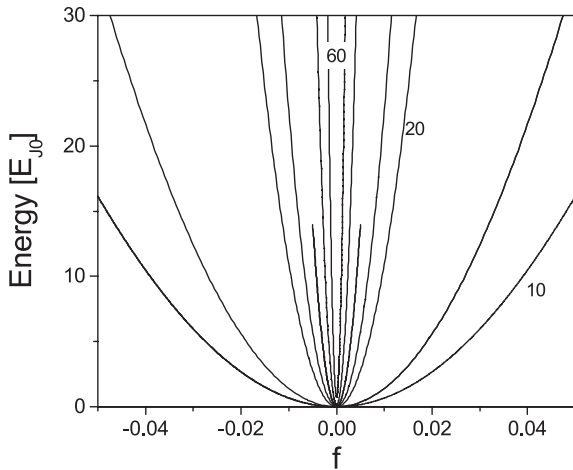


Fig. 2. Energy (in units of E_{J0}) as a function of frustration for different array sizes ($N = 10, 12, 20, 24, 30, 40, 60$) and without vortices.

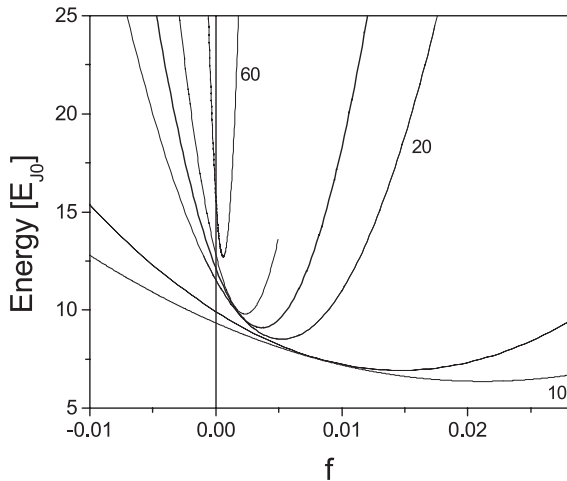


Fig. 3. Energy (in units of E_{J0}) as a function of frustration for different array sizes ($N = 10, 12, 20, 24, 30, 60$) and one vortex in the system.

sizes. It is clear the parabolic dependence with an increasing curvature as a function of sample size.

In the case of one vortex in the sample we started the simulations with a frustration of $f = 0$, and a phase configuration given by the arctangent model [8] for a vortex in the center of the system. Then similarly as before we change the frustration in small steps and let the system relax to the minimum of energy, checking in each step that the vorticity of the system remains equal to one. In Figure 3 we plot the results for these simulations. Again it is clear the parabolic dependence for the energy with an increasing curvature as increasing the sample size. Another interesting point to remark is the fact that the minimum for each parabola is not located in $f = 1/N^2$, frustration where the total magnetic flux is equal to one flux quantum in the system, but at larger frustrations. This is a clear effect of the sample boundaries that imposes the condition of no currents leaving the sample.

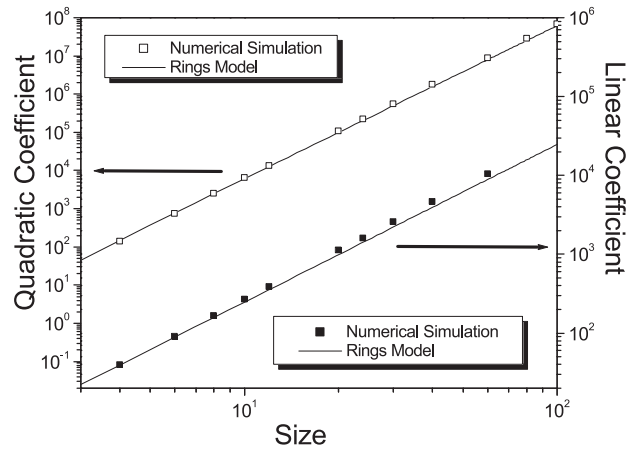


Fig. 4. Left axis: Quadratic coefficient. Symbols: results the simulation. Line: rings model. Right axis: Linear term. Open symbols: results from the simulation with $n_v = 1$. Line: Rings model.

For each of these curves ($n_v = 0, 1$) we have performed a linear square fit with a quadratic expression. In Figure 4 we plot the quadratic coefficient from the fits and the results from the rings model as a function of sample size. Also in the same figure we draw the linear coefficient obtained from the fit in the results of the simulations with one vortex, and the values obtained from the model. It is clear the excellent agreement between model and simulations specially in the quadratic term. The difference observed in the linear term is due to the simplification done in the model neglecting the radial junction contribution to the total energy. A simple adjustment of the energy within this model that can take into account this contribution is presented in Appendix B.

3.1 First critical field

For a given sample size the crossing between the curves of $n_v = 0$ and $n_v = 1$ defines the frustration where becomes energetically favorable the creation of a vortex excitation in the sample and can be defined as a *first critical field* for the system. In Figure 5 we plot these values for the case of the simulations and those obtained with the rings model as a function of sample size. The agreement between the model and the simulation in the whole range of sizes investigated spanning almost 2 orders of magnitude is remarkable. As expected the extrapolation to infinite systems gives a zero critical field and for a 2×2 system to $f = 1/2$.

4 Discussion and conclusions

Our results show that the magnetic field dependence of the ground state energy of Josephson junction arrays with open boundaries follow a parabolic dependence with a quadratic coefficient proportional to the fourth power of the size, for the case of zero and one vortex in the system.

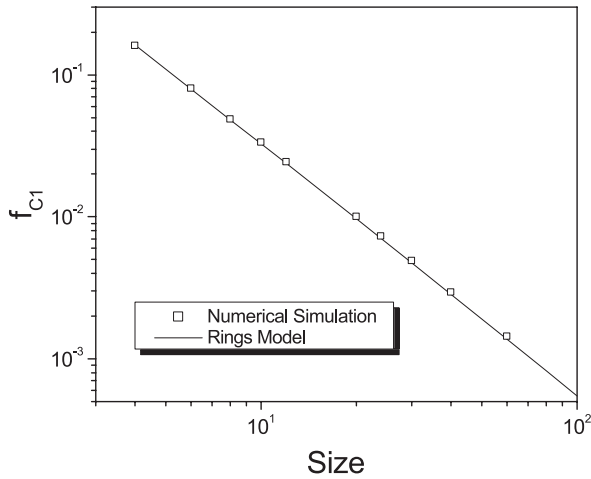


Fig. 5. First critical field as a function of sample size. Dots data obtained in the numerical simulations, line result from the rings model.

A simple rings model gives analytical expressions that reproduces with very good approximation the field and size dependence of the ground state energy. Size effects are clearly represented by the existence of a first critical field greater than the infinite limit $f_{C1} = 1/N^2$. These results made evident that influence of boundaries could not be neglected on considering vortex structures and phase transitions in Josephson junction arrays.

Appendix A

It is interesting to note that in the case of zero vortices in the system the expression (6) can be written in a closed form:

$$E_T(n_v = 0, f) = \frac{1}{2} \sin\left(\frac{f\pi}{2}\right)^{-2} \left[N^2 (1 - \cos(\pi f)) - N 4 \sin(\pi f/2) \sin(\pi N f/2) + 4 \cos(\pi f/2) (1 + \cos(\pi N f/2)) \right]. \quad (9)$$

Appendix B: Radial junctions correction

In the rings model presented in this work we have neglected the energy contribution from the *radial* junctions, those that interconnects successive concentric rings. This fact gives a systematic sub-estimation of the total energy as can be clearly seen in Figure 6. We can evaluate this extra energy for the state of one vortex in the system without magnetic field.

In each square ring the 2π phase change is equally distributed between all the junctions. This implies that in one side of the ring the phase can be expressed as $\theta(i, M) = -\frac{\pi}{4} + \frac{\pi}{2} \frac{i}{M-1}$, where M is the side size of the ring and $i : [0, M-1]$ is the node index within the ring.

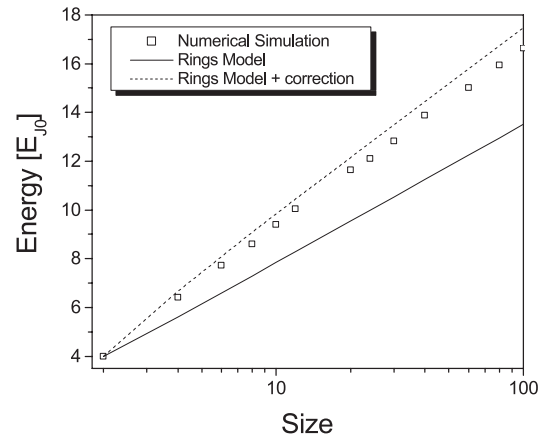


Fig. 6. Ground state energy obtained numerically (symbols), the rings model (full line), and rings model with correction (dashed line) as a function of sample size for one vortex in the center of the system and zero magnetic field.

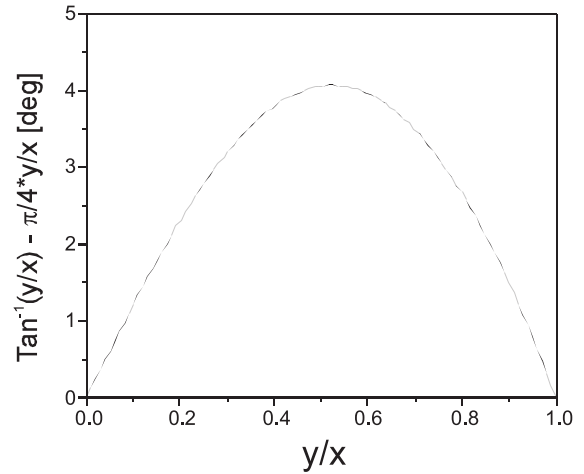


Fig. 7. Phase difference between the arctangent model and the rings model as a function of the node position defined as y/x .

In this way the total energy from the radial junctions can be expressed as:

$$E_R = \sum_{k=2}^{N/2} 4 \sum_{i=0}^{2k-3} \left[1 - \cos\left(\frac{\pi}{2} \left(\frac{i}{(2k-3)} - \frac{i+1}{(2k-1)} \right) \right) \right]. \quad (10)$$

Note that this expression gives an over-estimation for energy difference between the rings model and the true ground state. As soon as radial junctions are connected, the phase configuration does not represent a minimum of the total energy since is a state that violates the current conservation in each node.

Appendix C: Comparison between rings model and the arctangent model

A model that gives a valid phase configuration for a vortex located in the center of a infinite system is the so called

arctangent model [8]. This state is built setting the phase in node located in the coordinates $(x_{i,j}, y_{i,j})$ with the expression:

$$\theta(i, j) = \arctan\left(\frac{y_{i,j}}{x_{i,j}}\right). \quad (11)$$

In the case of finite systems this only gives a good approximation to the real state as border effects are not taken into account.

Although the arctangent model gives a much better phase configuration for the state of one vortex and zero frustration than the rings model, its extension to include the magnetic field dependence is not trivial. On the other hand our model easily takes into account this dependence.

In Figure 7 we have plotted the phase difference between the arctangent model and our *rings* model as a function of the node position y/x . This clearly shows that both models coincides on symmetry axis for the square array and the maximal difference is about 4 degrees. This is a further proof that our state is very close to local energy minimum.

References

1. P. Martinoli, Ch. Lehman, J. Low Temp. Phys. **118**, 699 (2000); R.S. Newrock, C.J. Lobb, U. Geigenmüller, M. Octavio, Solid State Phys. **54**, 263 (2000)
2. Y.-H. Li, S. Teitel, Phys. Rev. Lett. **66**, 3301 (1991); E.A. Jagla, C.A. Balseiro, Phys. Rev. B **52**, 4494 (1995)
3. L.J. Geerligs, M. Peters, L.E.M. de Groot, A. Verbruggen, J.E. Mooij, Phys. Rev. Lett. **63**, 1754 (1989)
4. H.S.J. van del Zant, H.A. Rijken, J.E. Mooij, J. Low Temp. Phys. **29**, 289 (1990)
5. T.J. Hagenaars, J.E. van Himbergen, J.V. José, P.H.E. Tiesinga, Phys. Rev. B **53**, 2719 (1996)
6. T.C. Halsey, Phys. Rev. B **31**, 5728 (1985); J.P. Straley, G.M. Barnett, Phys. Rev. B **48**, 3309 (1993)
7. M.R. Beasley, J.E. Mooij, T.P. Orlando, Phys. Rev. Lett. **42**, 1165 (1979)
8. C.J. Lobb, David W. Abraham, M. Tinkham, Phys. Rev. B **27**, 150 (1982)